Supplemental Material can be found at:
http://www.jbc.org/content/suppl/2011/05/11/M110.167544.DC1.html

THE JOURNAL OF BIOLOGICAL CHEMISTRY VOL. 286, NO. 26, pp. 23178–23188, July 1, 2011
© 2011 by The American Society for Biochemistry and Molecular Biology, Inc. Printed in the U.S.A.

Caspase-3 Cleavage Links δ-Catenin to the Novel Nuclear Protein ZIFCAT*[S]

Received for publication, August 5, 2010, and in revised form, May 10, 2011 Published, JBC Papers in Press, May 11, 2011, DOI 10.1074/jbc.M110.167544

Dongmin Gu[‡§], Nam Ky Tonthat[‡§], Moonsup Lee[‡§], Hong Ji[§], Krishna P. Bhat[¶], Faith Hollingsworth[¶], Kenneth D. Aldape[¶], Maria A. Schumacher[‡§], Thomas P. Zwaka[‖], and Pierre D. McCrea[‡§1]

From the [‡]Program in Genes and Development, University of Texas Graduate School of Biomedical Sciences, Houston, Texas 77030, the [§]Department of Biochemistry and Molecular Biology and [¶]Department of Pathology, University of Texas M. D. Anderson Cancer Center, Houston, Texas 77030, and the [‖]Department of Molecular and Cellular Biology, Baylor College of Medicine, Houston, Texas 77030

δ-Catenin is an Armadillo protein of the p120-catenin subfamily capable of modulating cadherin stability, small GTPase activity, and nuclear transcription. From yeast two-hybrid screening of a human embryonic stem cell cDNA library, we identified δ-catenin as a potential interacting partner of the caspase-3 protease, which plays essential roles in apoptotic as well as non-apoptotic processes. Interaction of δ-catenin with caspase-3 was confirmed using cleavage assays conducted *in vitro*, in *Xenopus* apoptotic extracts, and in cell line chemically induced contexts. The cleavage site, a highly conserved caspase consensus motif (DELD) within Armadillo repeat 6 of δ-catenin, was identified through peptide sequencing. Cleavage thus generates an amino-terminal (residues 1–816) and carboxyl-terminal (residues 817–1314) fragment, each containing about half of the central Armadillo domain. We found that cleavage of δ-catenin both abolishes its association with cadherins and impairs its ability to modulate small GTPases. Interestingly, 817–1314 possesses a conserved putative nuclear localization signal that may facilitate the nuclear targeting of δ-catenin in defined contexts. To probe for novel nuclear roles of δ-catenin, we performed yeast two-hybrid screening of a mouse brain cDNA library, resolving and then validating interaction with an uncharacterized KRAB family zinc finger protein, ZIFCAT. Our results indicate that ZIFCAT is nuclear and suggest that it may associate with DNA as a transcriptional repressor. We further determined that other p120 subfamily catenins are similarly cleaved by caspase-3 and likewise bind ZIFCAT. Our findings potentially reveal a simple yet novel signaling pathway based upon caspase-3 cleavage of p120-catenin subfamily members, facilitating the coordinate modulation of cadherins, small GTPases, and nuclear functions.

The means by which biological signals produce coordinate effects in varying cellular compartments is relevant to the execution of many developmental and pathological processes, and often involves events that take place at the plasma membrane, in the cytoplasm, and in the nucleus. Canonical Wnt signaling, for example, generally occurs upon Wnt-ligand binding to cell surface receptors (*e.g.* Frizzled and Lrp5/6), facilitating Dishevelled-mediated inhibition of the β-catenin destruction complex (composed of Axin, GSK-3β, APC, etc.). This results in cytoplasmic and nuclear accumulation of β-catenin and in activation of canonical Wnt/β-catenin target genes (1, 2). The membrane-spanning Notch receptors, on the other hand, are protease-cleaved upon the binding of ligands such as Delta or Jagged, such that the intracellular portion of Notch is liberated to enter the nucleus, associate with the CSL transcription factor complex (CBF1, Su(H), Lag-1), and modulate specific gene targets (3). Both the Wnt and Notch pathways participate in multiple developmental/cellular processes and, when abnormally regulated, contribute to human disease, including cancer (4, 5).

Classic cadherins are trans-membrane proteins best known to mediate cell-cell adhesion. Together with catenins, which associate with cadherin intracellular tails and indirectly and dynamically with the actin cytoskeleton, cadherins play essential roles in establishing adherens junctions, thereby participating in tissue architecture and polarity, morphogenesis, and cell identity (6–8). Physiologic or deregulated alterations in adherens junction function is associated with normal or disease processes, respectively, the latter including metastasis (9, 10). Interestingly, cadherins and catenins are targeted by proteases, yielding varied downstream outcomes. Proteases identified include members of the caspase family (11–21), widely known for their roles in apoptosis but, importantly, essential also in many non-apoptotic events (22, 23). Although the causation and consequences of cadherin and catenin proteolysis remain under study (24–27), with regard to epithelial apoptosis, the dismantling of cell-cell contacts probably assists dying cells in detaching themselves and/or in being removed by surrounding or scavenger cells (28). Given that adherens junctions are dynamic structures, as made evident in development and wound repair (etc.), the regulated proteolysis of catenins may permit rapid junctional (as well as small GTPase) responses to upstream signaling events, with the generated catenin fragments conceivably having further gene-regulatory activities (11).

δ-Catenin is a member of the p120 subclass of catenins, which further includes p120-, ARVCF-, and p0071-catenin

* This work was supported, in whole or in part, by National Institutes of Health Grant RO1 GM52112 (to P. D. M.), and assistance with DNA sequencing and other core facilities was provided by National Institutes of Health, NCI, Core Grant CA-16672 (to M. D. Anderson Cancer Center). This work was also supported by a Texas ARP Grant and March of Dimes Grant 1-FY-07-461-01 (to P. D. M.).

[S] The on-line version of this article (available at http://www.jbc.org) contains supplemental Figs. 1 and 2.

[1] To whom correspondence should be addressed. E-mail: pdmccrea@mdanderson.org.

Downloaded from www.jbc.org at HAM-TMC Library, on January 31, 2013

(29, 30). The central region of δ-catenin is composed of nine Armadillo repeats, which together form a helix of α-helices engaging in multiple protein interactions. Established functions of p120 subfamily members include their binding to cadherin juxtamembrane regions (whereas β-catenin binds a more distal site), where they stabilize the larger adhesion complex by reducing its rate of internalization (31). In addition, δ-catenin associates with small GTPases and/or their effectors, enabling the production or maintenance of discrete actin-dependent outgrowths, such as dendritic projections in neurons (32–35). δ-Catenin is further required in certain collective cell processes, apparently including amphibian gastrulation, via the modulation of Rho/Rac (36). Aside from its roles at the plasma membrane (adherens junctions) and in the cytoplasm (small GTPases), δ-catenin is intriguingly also present within nuclei in some tissues (37). For example, in the context of the neural-muscular junction, δ-catenin binds the transcriptional regulator Kaiso, which additionally binds p120-catenin (38). In mammals, δ-catenin is predominantly expressed in neural tissues, with its loss leading to impaired cognition (39–41). In amphibians, δ-catenin exhibits a much wider expression pattern, reflected functionally in its above noted essential role in early development/gastrulation (36). From the perspective of human disease, abnormal expression of δ-catenin is associated with the progression of several carcinomas, including those of the prostate, lung, and breast (42–44).

In this study, we present evidence that δ-catenin is a novel substrate of caspase-3, generating a fragment that exhibits enhanced nuclear localization and binds a novel zinc finger transcription factor. We find that cleavage of δ-catenin both abolishes its association with cadherin and impairs its ability to modulate small GTPases. To probe potential nuclear roles of δ-catenin, we performed yeast two-hybrid screening from an adult mouse brain cDNA library, resolving and then validating interaction with an uncharacterized KRAB family zinc finger protein, ZIFCAT. Our results indicate that ZIFCAT is nuclear and that it is likely to associate with DNA and act as a transcriptional repressor. Last, we report that other p120 subfamily catenins are similarly cleaved by caspase-3 and likewise bind ZIFCAT. Our findings potentially reveal a simple and novel signaling pathway based upon caspase-3 cleavage of p120-catenin subfamily members, facilitating the coordinate modulation of cadherin, small GTPases, and nuclear functions.

EXPERIMENTAL PROCEDURES

Cell Culture, Immunofluorescence, and Luciferase Assays—HEK 293T, HeLa, and MDA-MB-435 cell lines were cultured following standard protocols and maintained in complete medium (Dulbecco's modified Eagle's medium (DMEM) with 10% fetal bovine serum (FBS) and antibiotics). Glioblastoma stem cells (GSC11) were grown in suspension as neurospheres or as monolayers on laminin-coated surfaces and maintained in neurobasal medium (DMEM/F-12, B27, with 10 ng/ml each of epidermal growth factor (EGF) and basic fibroblast growth factor). Plated cells were transiently lipofected with selected cDNA constructs according to the manufacturer's instructions (Lipofectamine 2000, Invitrogen) and cultured for 24–48 h prior to the next procedure(s). Immunofluorescence staining of cells was performed using standard methods, with 4% paraformaldehyde (Electron Microscopy Sciences) as fixative. Luciferase assays were according to the manufacturer's protocol, employing *Renilla* as a transfection control (Promega Dual-Luciferase® reporter assay).

Xenopus Apoptotic Extracts and Cell Death Detection ELISA—Apoptotic extracts were collected from *Xenopus* eggs using published protocols (45) and incubated with the Armadillo domain of δ-catenin (glutathione *S*-transferase (GST)-tagged) for the indicated periods at room temperature. Cleavage products were resolved by immunoblotting using GST antibody (Developmental Studies Hybridoma Bank). Puromycin and staurosporine were purchased from Calbiochem (catalog no. 178489) and applied to induce apoptosis at final concentrations of 0.5 and 20 ng/μl, respectively. Cytosolic nucleosomes resulting from chromatin breakage were quantified using an ELISA-based cell death detection kit following the manufacturer's protocol (Roche Applied Science).

Coupled Transcription/Translation and in Vitro Caspase-3 Cleavage Assays—cDNA constructs were transcribed/translated *in vitro* using the Promega TNT SP6 high yield wheat germ protein expression system. In some experimental contexts, Transcend tRNA was included in reactions to non-radioactively (biotin) label lysine residues of translated proteins. Following translation, 5 μl of the reaction mix was incubated with recombinant caspase-3 (BD Pharmingen) at 37 °C for 1 h.

Nuclear Fractionation, Immunoprecipitation, and Immunoblotting—Nuclear fractionation of 293T or HeLa cells followed published protocols (46). Standard procedures were used in immunoprecipitations from whole cell extracts or from diluted nuclear fractions, followed by immunoblotting. Streptavidin-horseradish peroxidase (HRP) (Promega) was employed to detect biotin-labeled proteins. Antibodies directed against Myc or HA epitope were purchased from the Developmental Studies Hybridoma Bank or Sigma-Aldrich (catalog no. H9658). δ-Catenin antibody 83-521 was reported previously (36). Other δ-catenin antibodies were obtained commercially from BD Biosciences (catalog no. 611536), Millipore (catalog no. 07-259), or Sigma-Aldrich (catalog no. C4989). Immunoblot band densities following scanning were quantified using AlphaEaseFC 6 software.

cDNA Cloning and Mutagenesis—Polymerase chain reactions were conducted to place restriction enzyme sites on each end of δ-catenin or ZIFCAT cDNA coding sequences. Directional subcloning then occurred through the use of restriction enzyme digestions and ligations into various vectors, followed by DNA sequence confirmation. Mutagenesis of δ-catenin Asp^{816} to Glu^{816} was performed using the manufacturer's protocol (QuikChange site-directed mutagenesis kit, Stratagene). Other constructs were reported previously (36, 47).

Rho and Rac Assays—HeLa cells were grown to ~70% confluence and transfected with the indicated cDNA constructs. 24 h post-transfection, complete medium was withdrawn and substituted with DMEM containing 0.1% FBS, and cells were

Downloaded from www.jbc.org at HAM-TMC Library, on January 31, 2013

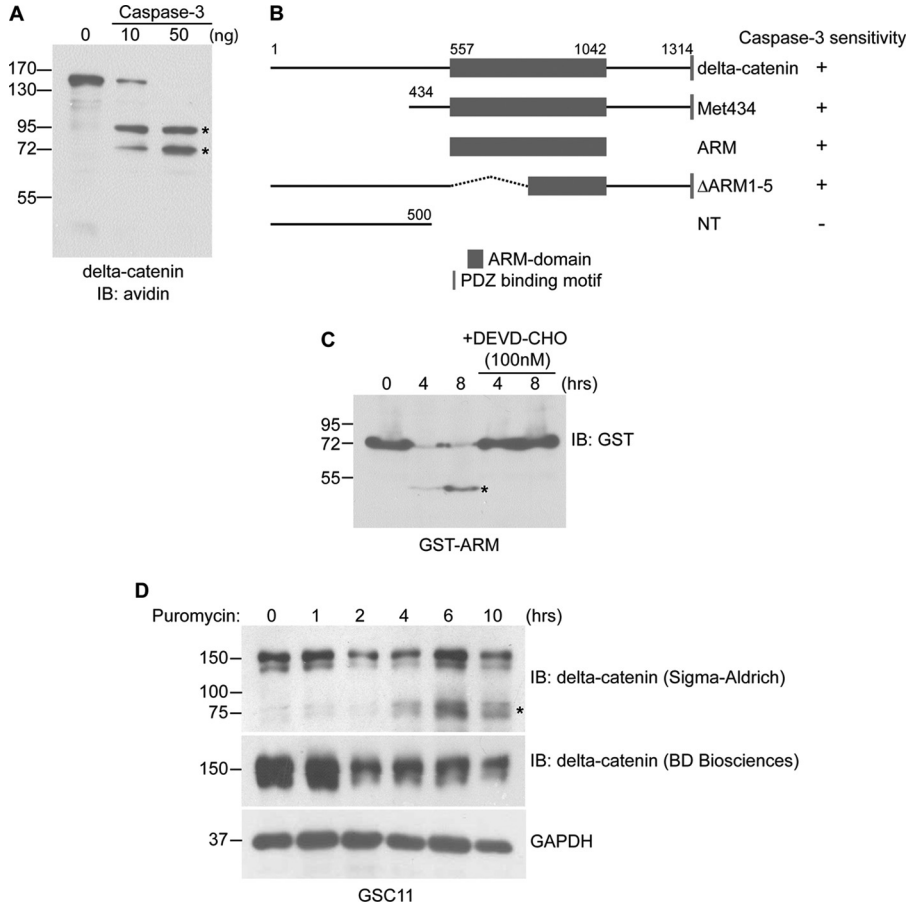

FIGURE 1. **δ-Catenin is cleaved by caspase-3 *in vitro* and in apoptotic extracts.** *A*, biotin-conjugated *Xenopus* δ-catenin was cleaved by recombinant active caspase-3 *in vitro*. Intact protein or cleaved fragments (labeled with *asterisks*) were visualized following SDS-PAGE, transfer to nitrocellulose, and immunoblotting (*IB*) using streptavidin-HRP. *B*, schematic illustration of varying *Xenopus* δ-catenin constructs to caspase-3 treatment *in vitro*. *C*, recombinant Armadillo domain of δ-catenin (GST fusion) was incubated in *Xenopus* egg extracts for the indicated times in the absence *versus* in the presence of DEVD-CHO, a specific inhibitor of caspase-3 and -7. Cleavage of δ-catenin (labeled with an *asterisk*) was detected by immunoblotting, using antibodies directed against GST. *D*, extracts from GSC11 cells treated with puromycin (0.5 ng/μl) were tested for endogenous human δ-catenin cleavage. An antibody recognizing the δ-catenin amino-terminal region (BD Biosciences) reproducibly showed a puromycin-dependent loss of full-length δ-catenin as expected (*middle*), whereas a carboxyl terminus-directed antibody (Sigma-Aldrich) resolved the appearance of a δ-catenin fragment migrating at a size consistent with caspase-3 generation of 817–1314 (labeled with an *asterisk*, *top*). GAPDH is included as a loading control.

starved for 16 h to minimize nonspecific serum effects. For the Rho assay, cells were further treated with lysophosphatidic acid for 5 min to enhance basal Rho levels. Cells were then lysed at 4 °C for 15 min in Mg^{2+} Lysis/Wash Buffer (Millipore), in the presence of protease and phosphatase inhibitors, and centrifuged for 10 min at 14,000 rpm. GTP-bound (active) Rho or Rac was pulled down from supernatants using 30 μg of Sepharose-conjugated recombinant Rho-binding domain or PAK-binding domain, respectively. Relative RhoA or Rac1 activities were determined by immunoblotting of pull-downs using antibodies directed against RhoA (Santa Cruz Biotechnology, Inc., Santa Cruz, CA) or Rac1 (BD Pharmingen).

In Vitro DNA Association Assay—*In vitro* genomic DNA association was assayed using established methods (48). In brief, selected ZIFCAT constructs were translated using the TNT system and mixed for 1 h at 4 °C in an optimized buffer with cellulose-conjugated calf thymus genomic DNA (Sigma-Aldrich). After extensive washing of the cellulose-DNA-protein complex, associated proteins were eluted, resolved on SDS-PAGE, and detected by immunoblotting.

RESULTS

δ-Catenin Is a Novel Caspase-3 Substrate—Yeast two-hybrid screening of a human embryonic stem cell cDNA expression library pointed to δ-catenin as a potential substrate of constitutively active caspase-3 (mcasp3rev), which was employed as the bait (results not shown). mcasp3rev spontaneously folds into its active conformation and binds target proteins but no longer cleaves them due to a C163S substitution (49). To begin to test this interaction's validity, we employed a classic *in vitro* assay wherein *Xenopus* δ-catenin was mixed with recombinant active caspase-3. δ-Catenin had been biotin-labeled on lysine residues, ensuring that all major fragments could be visualized through streptavidin-HRP immunoblotting. Remarkably, we observed significant cleavage at a low caspase-3 dose (10 ng), with complete cleavage occurring at higher doses (50 ng) (Fig. 1*A*). We then tested mouse δ-catenin, finding that it is likewise sensitive to caspase-3 treatment (results not shown). To map the region necessary for caspase-3 binding and cleavage, we collected additional *Xenopus* δ-catenin constructs and tested them using the same assay. Fig. 1*B* summarizes their

Downloaded from www.jbc.org at HAM-TMC Library, on January 31, 2013

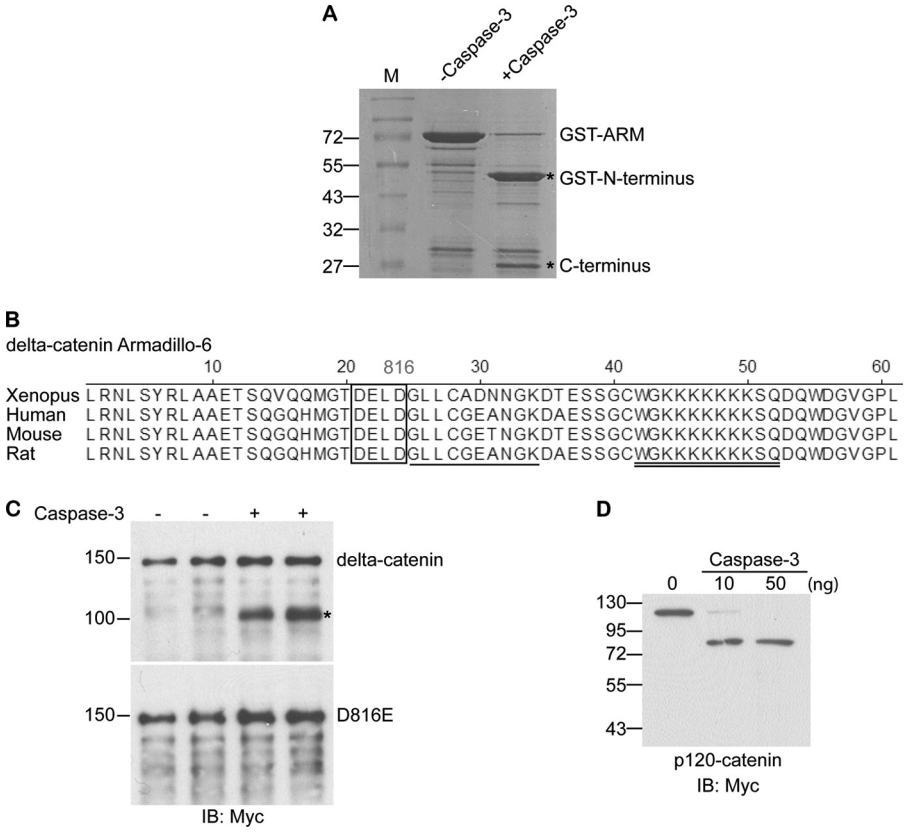

FIGURE 2. **Identification of caspase-3 consensus motif within δ-catenin.** *A*, recombinant Armadillo domain of δ-catenin was cleaved by active caspase-3 *in vitro*, with the resulting fragments resolved by SDS-PAGE and stained with Coomassie Brilliant Blue. A separate gel run in parallel was blotted onto a PVDF membrane, and the carboxyl-terminal δ-catenin band (labeled *C-terminus*) was excised for peptide sequencing. *B*, peptide sequencing of the δ-catenin carboxyl-terminal fragment identified the residues GLLCADNNGK (*underlined* is the corresponding rat sequence) and revealed the upstream caspase-3 tetrapeptide motif DELD. This site is highly conserved across multiple species. Note that the more downstream *double-underlined* residues WGKKKKKKKSQ represent a conserved nuclear localization sequence. *C*, mutation of the critical residue aspartate 816 to glutamate abolished δ-catenin susceptibility to active caspase-3 *in vitro* when compared side-by-side with the wild-type protein. An *asterisk* labels the partial cleavage product of wild-type δ-catenin. *D*, Myc-tagged p120-catenin is likewise an *in vitro* caspase-3 substrate as confirmed via immunoblotting (*IB*).

response to caspase-3 *in vitro*. The Armadillo domain of δ-catenin, and more specifically repeats 6–10, appeared to be the region of caspase-3 recognition. We next used an established *in vivo*-derived assay of caspase function (45). Apoptotic extracts harvested from *Xenopus* eggs were incubated with the bacterial expressed entire Armadillo domain of δ-catenin, which became markedly cleaved and apparently further metabolized (Fig. 1*C*).

Notably, the addition of DEVD-CHO (Calbiochem), a specific inhibitor for caspase-3 and -7, completely abolished this cleavage in apoptotic *Xenopus* extracts. To examine endogenous δ-catenin cleavage in mammalian cells, we screened six glioblastoma stem cell lines (results not shown), finding one (GSC11) that expressed δ-catenin at significant levels. Four independent antibodies confirmed δ-catenin migrating on SDS-PAGE as a ~150-kDa doublet (calculated molecular mass, 133 kDa). δ-Catenin was cleaved following the incubation of GSC11 cells with puromycin, a protein synthesis inhibitor and established apoptotic inducer (Fig. 1*D*) (50, 51). An antibody directed against the carboxyl-terminal region of δ-catenin reproducibly detected a cleavage fragment. In contrast, the amino-terminal fragment was not resolved employing proven antibodies from three different sources (also see below, and see "Discussion"). Such *in vivo* cleavage was likewise observed for Met^{434} δ-catenin, expressed exogenously in 293T cells (Fig. 4*D*). These findings together suggest that caspase-3 may be the predominant enzyme responsible for initial δ-catenin cleavage during apoptotic or potentially non-apoptotic events.

Caspase-3 Cleaves δ-Catenin at $DELD^{816}$ Consensus Motif—To identify the tetrapeptide motif for caspase-3 targeting, we performed *in vitro* cleavage as noted above, using the Armadillo domain of δ-catenin purified from *Escherichia coli*. Cleavage was confirmed by Coomassie Blue staining (Fig. 2*A*). A separate gel with equal loading was blotted onto a PVDF membrane, the peptide band was excised, and the first 10 amino-terminal residues were determined. Fig. 2*B* illustrates the GLLCADNNGK sequencing result, which in turn pointed to the upstream tetrapeptide motif $DELD^{816}$, a typical caspase-3 consensus site. Residue Asp^{816} probably represents position P1, the key amino acid for caspase-3 binding, after which peptide bond cleavage occurs. Upstream amino acids Asp, Glu, and Leu would then represent the P4, P3, and P2 residues, respectively, each contributing to caspase-3 recognition and association (52). It is notable that this caspase-3 site of δ-catenin is highly conserved across species (Fig. 2*B*). To verify the significance of Asp^{816}, we carried out site-directed mutagenesis, converting the native aspartate to glutamate, an amino acid that resembles aspartate in its chemical nature yet is

Downloaded from www.jbc.org at HAM-TMC Library, on January 31, 2013

resistant to caspase cleavage. The D816E mutant completely blocked caspase-3 cleavage *in vitro* compared with the wild-type δ-catenin (Fig. 2*C*). Intriguingly, the p120- and ARVCF-catenins also contain conserved predicted caspase-3 consensus sites within their Armadillo domains. These additional catenins are likewise sensitive to caspase-3 *in vitro*, suggesting that caspase-3 regulation of p120-catenin subfamily members may be a general phenomenon (Fig. 2*D*) (results not shown). Collectively, our *in vitro* and *in vivo* data strongly suggest that δ-catenin is a novel substrate of caspase-3 and is cleaved after the DELD^{816} motif.

Cleavage of δ-Catenin Abolishes Cadherin Binding—To probe for potential physiological relevance, we subcloned the two δ-catenin fragments formed as a result of caspase-3 cleavage and examined their ability to bind cadherin *in vitro* and in live cells. Hereafter we designate "1–816" to refer to the amino-terminal fragment (*Xenopus* δ-catenin amino acids 1–816), and "817–1314" to refer to the carboxyl-terminal fragment (*Xenopus* δ-catenin amino acids 817–1314). As expected, and employed as a positive control, full-length δ-catenin bound C-cadherin when translated and tested *in vitro*. In contrast, neither 1–816 nor 817–1314 displayed comparable immunoblot signals, suggesting that both of these fragments had greatly reduced capacities to bind cadherin (Fig. 3*A*). Next, we *in vitro* transcribed these cDNA constructs into capped mRNAs and injected them into one-cell stage *Xenopus* embryos, a classic approach used to test interactions with endogenous (or exogenous) proteins *in vivo*. Repeatedly, we observed a positive association between full-length δ-catenin with endogenous C-cadherin, a major cadherin mediating blastomere adhesion during early embryonic cleavage stages. Neither 1–816 nor 817–1314 produced a specific signal when compared with the IgG negative control pull-downs (Fig. 3*B*). These results suggest that caspase-3 cleavage of δ-catenin (and of p120- and ARVCF-catenins) prevents its association with cadherins. Given the recognized protective effects of bound p120-catenin subfamily members on cadherin stability, this may contribute to the known reduction of cadherin function following caspase activation.

Cleaved δ-Catenin Fragments Are Impaired in Rho and Rac Modulation—Rho and Rac are Ras family small G proteins that critically mediate actin dynamics and tissue morphogenesis (53). A prominent function of p120-catenin subfamily catenins, including δ-catenin, is their direct or indirect association and modulation of small GTPases, affecting their GTP- *versus* GDP-bound states (active *versus* inactive) (32). To test if the impact of δ-catenin upon Rho and Rac is lowered upon cleavage, we compared full-length *versus* 1–816 or 817–1314 (cleaved) constructs, evaluating Rho or Rac activity using Rho-binding domain or PAK-binding domain pull-down assays, respectively. Consistent with other reports (33, 36, 54, 55), expression of full-length δ-catenin in HeLa cells inhibited RhoA while partially activating Rac1 (Fig. 3, *C* and *D*). Both 1–816 and 817–1314, in contrast, failed to alter RhoA activity (Fig. 3*C*). With respect to Rac1, 1–816, as anticipated, lacked stimulatory or other effects, whereas unexpectedly, 817–1314 reproducibly displayed inhibitory, possibly dominant negative effects (Fig. 3*D*). These results suggest that caspase-3 cleavage of δ-catenin reduces or alters the modulation of small GTPases by δ-catenin, probably coincident and possibly in coordination with effects upon cadherin function.

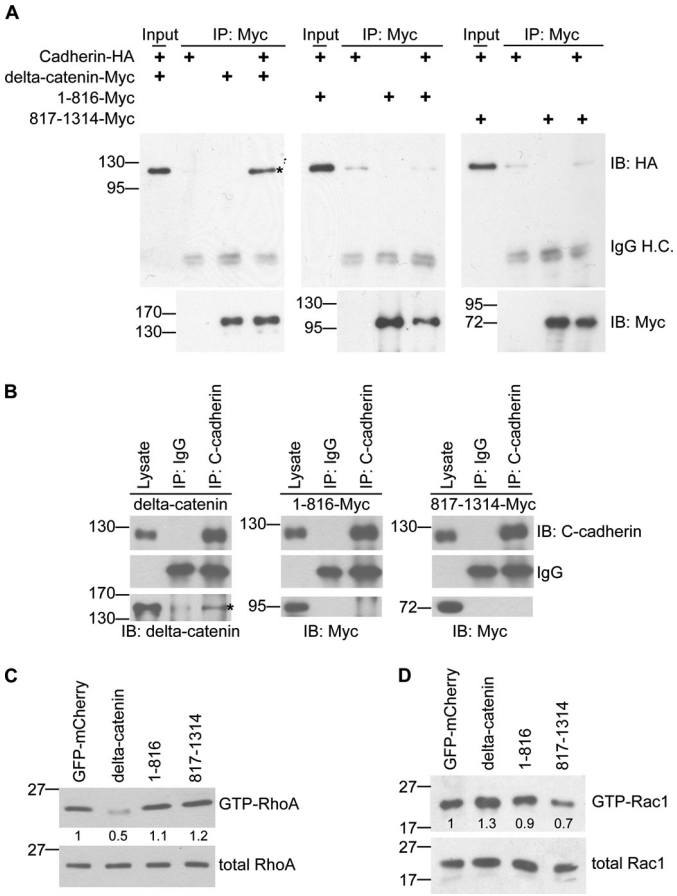

FIGURE 3. **Cleaved δ-catenin fragments fail to associate with cadherins and exhibit impaired small GTPase regulation.** *A*, selected constructs were translated *in vitro* and then incubated together using established conditions. Antibody against the Myc epitope was followed by Protein A/G beads, allowing immunoprecipitation (*IP*) of Myc-tagged δ-catenin proteins with (or without) associated C-cadherin. Immunoblotting (*IB*) using HA antibody indicated that C-cadherin associated with full-length δ-catenin but not the cleaved fragment 1–816 or 817–1314. IgG heavy chains were used as a loading reference. *B*, δ-catenin cDNA constructs were transcribed *in vitro* as capped mRNAs and then injected into *Xenopus* embryos for expression. Immunoprecipitates of endogenous C-cadherin from stage 12 gastrulating embryo extracts were resolved by SDS-PAGE and blotted for δ-catenin. Full-length δ-catenin displayed a positive association (labeled with an *asterisk*), in contrast to the cleaved fragment 1–816 or 817–1314 or the IgG controls. *C*, Rho activation was measured in extracts of HeLa cells transiently expressing selected δ-catenin constructs. Transfections were optimized to achieve maximal efficiency and monitored by GFP-mCherry expression. Full-length δ-catenin reduced the cellular level of active RhoA, whereas neither 1–816 nor 817–1314 displayed a significant impact relative to the control transfection. Numeric values represent the quantitations of GTP-RhoA (active) relative to total RhoA. *D*, Rac activation assays were conducted in a similar manner as in *C*, except that PAK-binding domain-agarose beads were used to pull down GTP-Rac (active), and Rac1 antibody was used for immunoblotting. In HeLa cells, full-length δ-catenin modestly but reproducibly increased the cellular levels of GTP-Rac1. 1–816 did not produce effects consistently different from the control. 817–1314 reproducibly showed a partial inhibition of Rac1 ($n > 3$ independent experiments). Numeric values represent the quantitations of GTP-Rac1 (active) relative to total Rac1.

An NLS[2] *within the δ-Catenin Armadillo Repeat 6 Enhances 817–1314 Nuclear Localization*—The 817–1314 fragment resulting from caspase-3 cleavage contains a WGKKKKK-

[2] The abbreviations used are: NLS, nuclear localization signal; UAS, upstream activation sequence; DBD, DNA binding domain.

Downloaded from www.jbc.org at HAM-TMC Library, on January 31, 2013

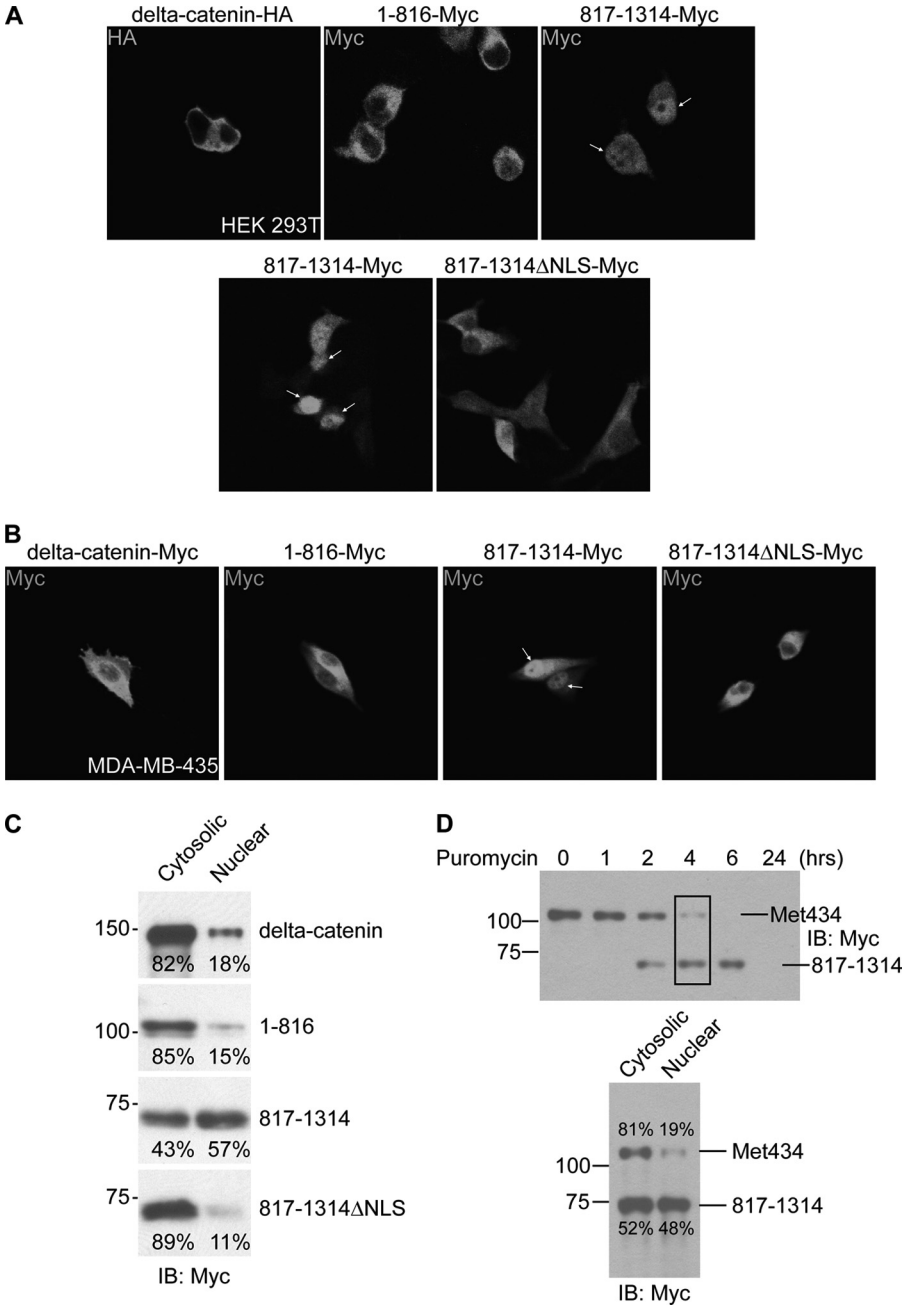

FIGURE 4. **The NLS within Armadillo repeat 6 enhances 817–1314 localization to nuclei.** *A*, confocal immunofluorescence localizations of various δ-catenin constructs. Full-length δ-catenin predominantly localizes to cell-cell borders and the cytoplasm in 293T cells, visualized via HA epitope staining. 1–816 is largely distributed within the cell cytosol, with lesser intensity at cell-cell borders. 817–1314, in contrast, displays a significant nuclear staining (marked with *arrows*), with additional cytosolic localization. Deletion of the NLS in 817–1314 reduced the presence of 817–1314 in the nucleus of 293T cells. *B*, subcellular localizations of δ-catenin constructs in MDA-MB-435 melanoma cells. *C*, cytosolic-nuclear fractionation of 293T cells followed by immunoblotting (*IB*) indicates that δ-catenin and 1–816 largely distribute to the cytosolic fraction, whereas 817–1314 exhibits a larger nuclear presence. Deletion of the NLS from 817–1314 efficiently redistributed the resulting construct to the cytosol. *D*, 293T cells transfected with the Met^{434} δ-catenin construct were treated with puromycin (0.5 ng/μl). Whole-cell extracts (obtained 4 h after treatment) were separated by cytosolic-nuclear fractionation and subject to Myc immunoblotting. Given that the Myc epitope was present at the δ-catenin carboxyl terminus, the nuclear enrichment of 817–1314 was confirmed relative to Met^{434} (*bottom*).

KKSQ sequence element previously demonstrated to possess nuclear localization activity (56) (see also Fig. 2*B*). To test if the NLS might contribute to the nuclear entry of 817–1314, epitope-tagged δ-catenin constructs were transiently expressed in various cell types, and this was followed by confocal immunofluorescence visualization. As shown in Fig. 4*A* using 293T cells, full-length δ-catenin appeared concentrated near cell-cell borders, with residual staining in the cytoplasm. Lacking the ability to bind cadherin, 1–816 was instead more diffusely localized in the cytosol. Likewise, in contrast to full-length δ-catenin, but also differing from 1–816, prominent localization to nuclei was observed for 817–1314, with additional cytosolic presence. Results from MDA-MB-435 melanoma cells (Fig. 4*B*), MDA-MB-231

Downloaded from www.jbc.org at HAM-TMC Library, on January 31, 2013

breast cancer cells (results not shown), and Neuro-2a neuroblastoma cells (results not shown) were consistent with observations from 293T cells. To test if the nuclear localization of 817–1314 required the NLS, we removed an amino-terminal region of 28 amino acid residues that included the WGKKKKKKKSQ element. When compared with 817–1314, removal of the NLS placed a much greater proportion of the resulting construct in the cytoplasm (Fig. 4, *A* and *B*). Next, we employed biochemical fractionation to better quantify the constructs' intracellular distribution. As shown in Fig. 4*C*, a prominent portion of 817–1314 localized to the nuclear fraction (57% of 100%), as distinguished from full-length δ-catenin (18%), 1–816 (15%), or 817–1314ΔNLS (11%). Similar results were obtained for 817–1314 in 293T cells subject to puromycin-induced cell death (Fig. 4*D*). Thus, our resolved caspase-3 cleavage of δ-catenin generates a fragment (817–1314) that becomes enriched in the nucleus, leaving open the possibility that 817–1314 has nuclear roles.

ZIFCAT Is a Novel KRAB Zinc Finger Protein Associating with δ-Catenin and ARVCF—The localization of 817–1314 encouraged us to test for potential functions of δ-catenin in the nucleus. Using *Xenopus* δ-catenin as bait, we performed a second yeast two-hybrid screen, this time employing an adult mouse brain cDNA library (Hybrigenics, Inc.). Because full-length δ-catenin exhibited autoactivation, we chose a δ-catenin construct deleted of its amino terminus (intact Armadillo and carboxyl-terminal domains). A total of 159 clones were obtained, representing 27 distinct potential interactions, including known associations with cadherins and Erbin (internal positive controls). Our screen was not saturating given that additional known interactions were not resolved. Intriguingly, the best rated interaction (Hybrigenics, Inc.) included 11 independent clones encoding a novel KRAB (Krüppel-associated box) zinc finger protein (2610008E11Rik) (Fig. 5*A*). KRAB zinc finger proteins feature a carboxyl-terminal zinc finger region that binds DNA and an amino-terminal KRAB motif associating with transcriptional cofactors (57). We termed this resolved novel protein ZIFCAT (zinc finger protein associating with catenins) (supplemental Fig. 2). As deduced from the 11 yeast two-hybrid ZIFCAT clones obtained, the minimal interacting sequence with δ-catenin included zinc finger repeats 6–8. Intriguingly, ZIFCAT was once again resolved in a parallel yeast two-hybrid screen aimed at identifying novel ARVCF-catenin interactions (results not shown) (Hybrigenics, Inc.). Based simply on the yeast two-hybrid clones resolved, the minimal ZIFCAT-interacting sequence associating with ARVCF likewise appears to include a similar (perhaps larger) zinc finger region. Thus, ZIFCAT was suggested to employ its zinc finger domain to bind δ- and ARVCF-catenin, the same region that might be anticipated to bind DNA.

To test the resolved yeast two-hybrid interactions, we performed *in vitro* binding assays as described earlier. Full-length δ-catenin bound to ZIFCAT *in vitro*. 817–1314, which is generated by caspase-3 cleavage and displays nuclear localization, also bound ZIFCAT (Fig. 5*B*). We failed, in contrast, to observe a positive association of ZIFCAT either with 1–816, with the isolated Armadillo domain of δ-catenin, or with the δ-catenin amino-terminal domain (results not shown). We then confirmed the *in vitro* interaction between ARVCF and ZIFCAT following a similar strategy but using ARVCF fused to maltose-binding protein and purified from *E. coli* (results not shown). Lacking antibodies against endogenous ZIFCAT, we next sought to resolve an interaction *in vivo* with full-length δ-catenin. This proved challenging because although ZIFCAT is predominantly nuclear (see also Fig. 6*A*), the majority of full-length δ-catenin or ARVCF remains at cell-cell contacts in complex with cadherins or cadherin-free within the cytoplasm, where it acts upon small GTPases. Given that our evidence pointed to a potential nuclear role of 817–1314, we co-transfected 817–1314 with ZIFCAT. As anticipated, co-immunoprecipitation from 293T nuclear fractions clearly confirmed the association of 817–1314 with ZIFCAT (Fig. 5*C*). We further wished to test for an *in vivo* association of ARVCF-catenin with ZIFCAT. Not knowing the precise caspase-3 cleavage site(s) within ARVCF or its validated endogenous NLS, we employed a different strategy, fusing an amino-terminal ectopic NLS to full-length ARVCF. This notably increased the presence of ARVCF in the nucleus (results not shown) and allowed us to resolve an association with ZIFCAT (Fig. 5*D*). Our results together indicate that two distinct p120-catenin subfamily members, δ- and ARVCF-catenin, each associate with ZIFCAT. Under physiologic circumstances involving caspase-3, we conjecture that a resulting fragment (such as 817–1314) is more likely to enter the nucleus and associate with ZIFCAT than the corresponding full-length catenin.

ZIFCAT Associates with Chromosomal DNA and May Act as a Transcriptional Repressor—To gain further insight into ZIFCAT, we examined its sub-cellular localization. As expected, HA-tagged ZIFCAT localized strongly to the nuclei of HeLa or 293T cells (Fig. 6*A*) (results not shown). We next tested if ZIFCAT associates with genomic DNA *in vitro*, using an established assay (48). Here, full-length ZIFCAT or a ZIFCAT construct lacking the amino-terminal 169 residues, including the KRAB domain (ZIFCAT-ZF), was co-incubated with cellulose-conjugated genomic DNA purified from calf thymus. Both constructs associated with the genomic DNA, whereas in contrast, this association was largely lost when the carboxyl-terminal 497 residues, including the zinc finger region of ZIFCAT, were removed (ZIFCATΔZF, Fig. 6*B*). Our data are thus consistent with the possibility that ZIFCAT associates directly or indirectly with DNA through its zinc finger repeats and, speculatively, exerts gene regulatory functions via KRAB domain co-factors, such as KAP1 (KRAB-associated protein 1) (58).

As an initial test of whether ZIFCAT might modulate gene transcription, we utilized the Gal4-UAS-luciferase system, wherein constructs of ZIFCAT were fused to the DNA binding domain (DBD) of Gal4, and their activity was tested by co-transfection in HeLa or 293T cells, followed by a luciferase assay. In this artificial setting, Gal4DBD mediates an interaction with the UAS sequence element present on the reporter construct, thereby bringing ZIFCAT into close proximity with the promoter governing luciferase activity. Repression was reproducibly observed with Gal4DBD-ZIFCAT or the Gal4DBD-ZIFCATΔZF mutant lacking the carboxyl-termi-

Downloaded from www.jbc.org at HAM-TMC Library, on January 31, 2013

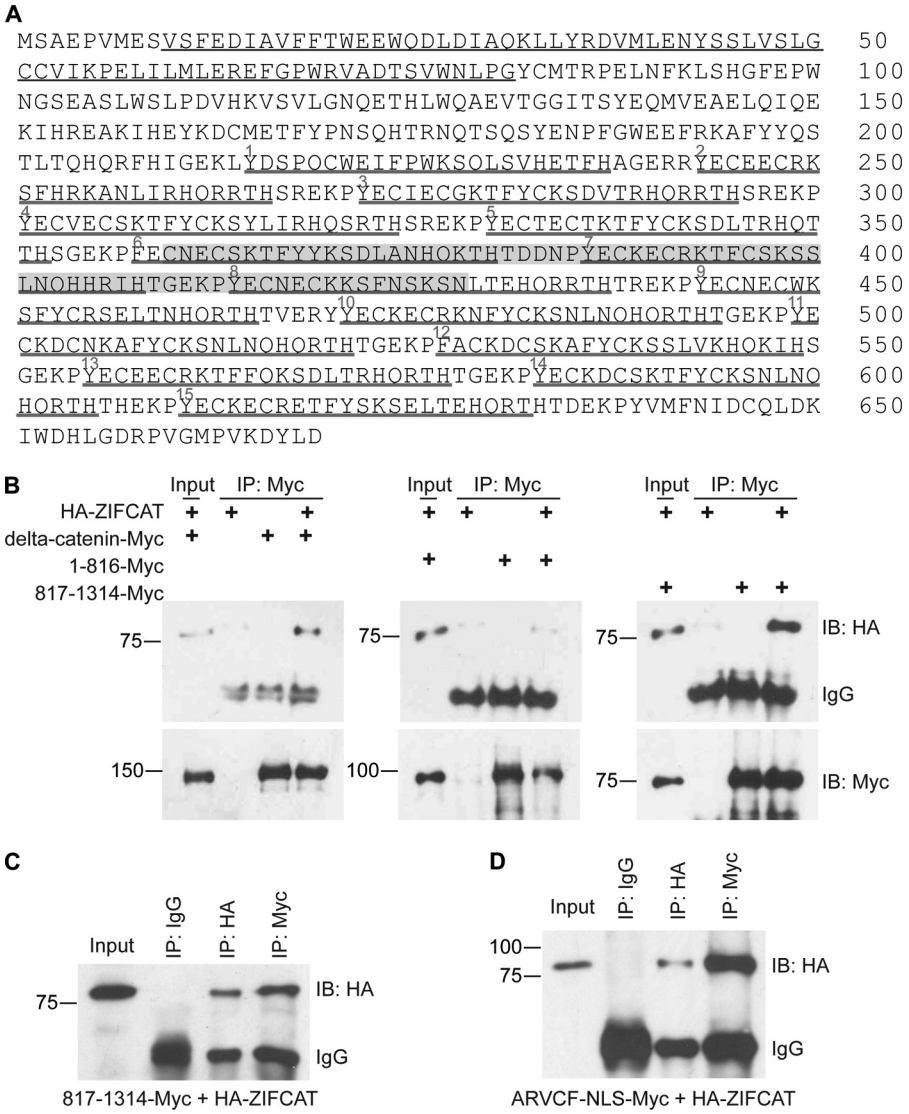

FIGURE 5. **ZIFCAT is a novel KRAB zinc finger protein associating δ- and ARVCF-catenin.** *A*, primary amino acid sequence of ZIFCAT. *Underlined* is the amino-terminal KRAB domain (xxx–yyy amino acids) and both numbered and *underlined* are the 15 C_2H_2 type zinc finger repeats occupying approximately two-thirds of ZIFCAT. *Shaded* residues comprise the minimal region deduced from yeast two-hybrid screening that associates with δ-catenin. *B*, 817–1314, found to result from caspase-3 cleavage, is sufficient to bind ZIFCAT *in vitro*. Selected constructs were translated *in vitro* and incubated together. Myc antibody followed by Protein A/G beads was used to immunoprecipitate (*IP*) δ-catenin proteins. Immunoblotting (*IB*) with HA antibody indicated that ZIFCAT associates *in vitro* with full-length δ-catenin (*left*) or 817–1314 (*right*) but not with 1–816 (*middle*) relative to control precipitations. *C*, 817–1314 associates with ZIFCAT in 293T cells. Myc-tagged 817–1314 and HA-tagged ZIFCAT were co-transfected into 293T cells. Myc antibody was employed to precipitate 817–1314, with HA immunoblotting confirming the association of 817–1314 with ZIFCAT. *D*, ARVCF likewise associated with ZIFCAT *in vivo*. Experimental conditions were as for *C*, except that NLS-Myc-tagged ARVCF was employed for co-transfection with ZIFCAT.

nal 497 residues, including the zinc finger region. Such effects were not observed for Gal4DBD alone or for HA-tagged ZIFCAT (negative controls) (Fig. 6*C*). Our results suggest a model where ZIFCAT gene activity may depend upon the zinc finger region for DNA association (see also Fig. 5*A*) and the amino-terminal region (probably the KRAB domain) for recruitment of transcriptional co-factors/co-repressors (57).

Finally, to probe for a functional interplay between ZIFCAT and δ-catenin (or ARVCF-catenin) in the context of this Gal4-UAS-luciferase system, we co-expressed δ-catenin (or ARVCF-catenin) with Gal4DBD-ZIFCAT. As seen in Fig. 6*D*, no significant changes followed such co-expression. This was perhaps to be expected because our data had already indicated that δ-catenin as well as ARVCF-catenin bind the zinc finger region of ZIFCAT, whereas the Gal4DBD-ZIFCAT construct no longer requires this domain for DNA association (imparted instead by the Gal4DBD fusion). *In vivo*, we conjecture that nuclear δ- or ARVCF-catenin or, more likely, caspase-3 fragments, such as 817–1314, displace ZIFCAT from its presently unknown consensus binding sites in promoter/enhancer DNA, relieving ZIFCAT-mediated gene repression.

DISCUSSION

Apoptosis or Programmed Cell Death Is a Physiologically Controlled Process of Cell Suicide—Activated caspases cleave specific cellular substrates, with dying cells presenting characteristic molecular and morphological features (59, 60). It has

Downloaded from www.jbc.org at HAM-TMC Library, on January 31, 2013

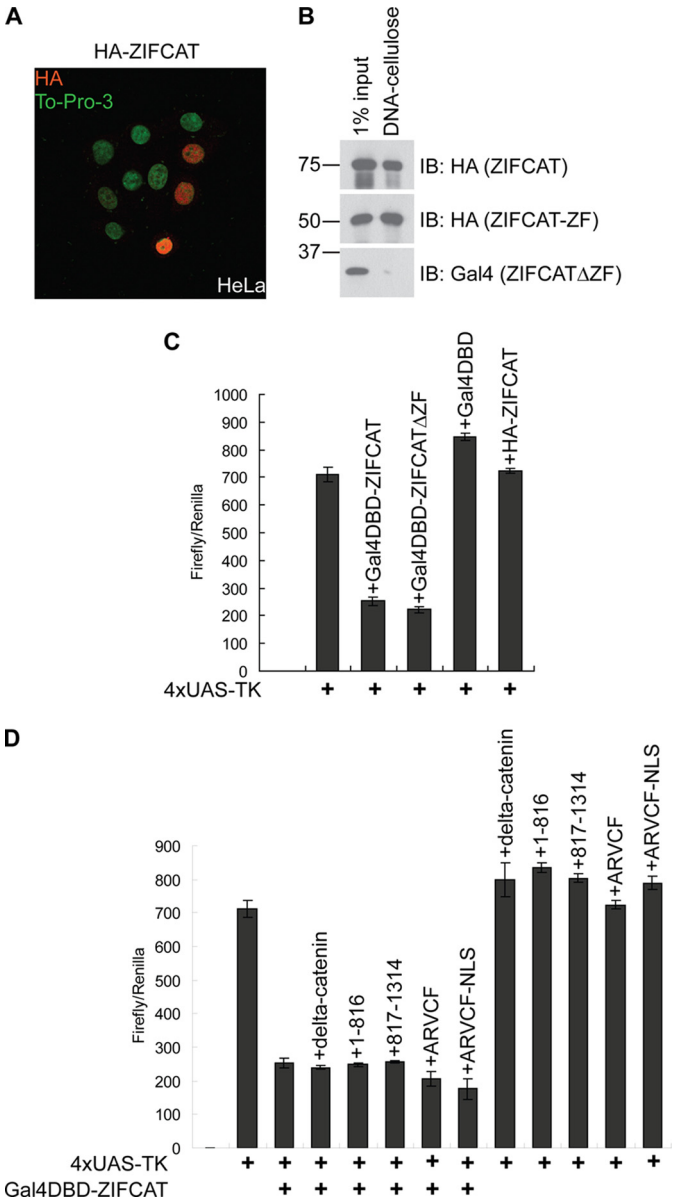

FIGURE 6. **ZIFCAT is a DNA-associating nuclear protein and represses UAS-luciferase activity.** *A*, HA immunofluorescence (*orange*) of ZIFCAT in HeLa cells, displaying a strong overlap with the To-Pro-3 nuclear counterstain in *green*. *B*, ZIFCAT associates with DNA through its zinc finger region. Selected constructs were translated *in vitro* and incubated with cellulose-conjugated calf thymus genomic DNA. After extensive washing, bound proteins were eluted and immunoblotted with the indicated antibodies. Full-length ZIFCAT as well as the region of ZIFCAT containing its zinc fingers (*ZIFCAT-ZF*) displayed positive DNA association, whereas the ZIFCAT mutant containing the KRAB but not the zinc finger domain (*ZIFCATΔZF*) lacked this interaction. *C*, the amino-terminal region of ZIFCAT represses UAS-luciferase activity. Selected constructs were fused to the Gal4 DNA binding domain, which promotes DNA association with UAS sequence elements residing within a standard thymidine kinase (*TK*)-luciferase reporter construct. Full-length ZIFCAT and the mutant lacking the zinc finger region repressed the expression of thymidine kinase-luciferase. Serving as negative controls, Gal4DBD or HA-tagged ZIFCAT (not recruited to the reporter's promoter) did not achieve significant inhibitory effects. Luciferase assays were repeated three times or more in HeLa or 293T cells, with one representative experiment being shown. *D*, neither δ- nor ARVCF-catenin has a notable impact upon the transcriptional repression conferred by Gal4DBD-ZIFCAT. δ- and ARVCF-catenin constructs were co-transfected with the TK-luciferase reporter in the presence or absence of Gal4DBD-ZIFCAT. Relative to the repressed state conferred by Gal4DBD-ZIFCAT expression alone (*lane 2*), no significant relief or repression was observed (*lanes 3–7*). Luciferase assays were reproduced three times or more using *Renilla* as the internal control, with one representative experiment being shown.

been long appreciated that caspases have many roles apart from apoptosis, such as in immune defense, proliferation, fate determination, terminal differentiation, cell migration, and neurodegeneration. The mechanisms by which caspases exert these non-apoptotic functions are still under active investigation yet probably relate to their temporally, spatially, or quantitatively controlled enzymatic activations (22, 23).

In this study, we present data indicating that δ-catenin is a novel substrate for caspase-3. δ-Catenin interacted with caspase-3 in yeast two-hybrid screening and was also shown to be cleaved by caspase-3 *in vitro* and in apoptotic cell extracts. This response may be conserved across the p120 subfamily of catenin proteins because p120-catenin also showed sensitivity to caspase-3 *in vitro*. Considering that caspase-3 is best known as an "executioner" caspase in the apoptotic cascade, one could imagine that δ-catenin may exert effects within cell death programs. Indeed, in independent work, exogenous δ-catenin expression resulted in limited cell death in NIH 3T3 cells (61). Conversely, however, δ-catenin has been reported to have prosurvival activities in prostate adenocarcinoma cells (43) and elicited feedback suppression of Pax6-induced apoptosis in HeLa cells (62). In our present study employing a cell death ELISA method, we did not observe significant increases or decreases in chromatin breakage upon δ-catenin expression (supplemental Fig. 1). Likewise, neither full-length δ-catenin nor the D816E, 1–816, or 817–1314 constructs protected HeLa cells from staurosporine- or puromycin-induced apoptosis. Perhaps prosurvival/proapoptotic effects may be context-dependent (*e.g.* we used *Xenopus* δ-catenin in our transfections rather than mouse or human constructs). Although *Xenopus* and murine δ-catenin are highly homologous (~90% identity), sequence divergences do exist, as might alternative splicing events. Further, we employed staurosporine and puromycin as potent general cell death inducers, whereas Pax6 expression would probably have more defined apoptotic roles. Ultimately, more sensitive gain/loss of function assays in additional systems may be required to reach a definitive conclusion regarding the role of δ-catenin in apoptosis.

The caspase-3 cleavage of δ-catenin potentially abolishes its binding to cadherins because the resulting fragments failed to co-immunoprecipitate with C-cadherin when expressed *in vitro* or *in vivo*. In GSC11 cells, where an antibody directed against the carboxyl-terminal region of δ-catenin reproducibly detected the presence of 817–1314 (especially upon apoptosis induction), we failed to observe 1–816, employing amino terminus-directed antibodies from three different sources. Thus, 1–816 appears to be more rapidly metabolically degraded following its generation. In that classic cadherins and some catenins are targeted during apoptotic events (11–21), cleavage of δ-catenin in this context may assist in orchestrating the disassembly of adherens junctions, where cadherins are known to be endocytosed following the disassociation of p120-catenin subfamily members. Additionally, as noted earlier, since caspases further participate in non-apoptotic processes, such modulation of cadherin levels and functions may instead have other physiologic outcomes, such as transitions to less adhesive and more motile cell phenotypes.

Downloaded from www.jbc.org at HAM-TMC Library, on January 31, 2013

Another recognized role of p120 subfamily catenins is their modulation of small GTPases (32). In our experimental setting, δ-catenin lost the ability to inhibit RhoA following its cleavage, with neither 1–816 nor 817–1314 exhibiting inhibitory activity. Regarding Rac1, whereas 1–816 and 817–1314 displayed no stimulatory activity in contrast to that of full-length δ-catenin, 817–1314 exhibited partial inhibitory effects. Rho and Rac contribute to a myriad of cellular processes, prominently including cytoskeletal organization and function (53). It is thus conceivable that caspase-3 cleavage of δ-catenin, probably in concert with that of other p120 subfamily members, is relevant to cell morphological changes in both apoptotic and non-apoptotic settings.

Caspase-3 cleaves Armadillo repeat 6 of δ-catenin. Because the NLS of δ-catenin resides only 18 amino acids downstream of this cleavage site, it may become more exposed and possibly account for the observed stronger nuclear localization of 817–1314 relative to full-length δ-catenin. Interestingly, an earlier report indicated the localization of δ-catenin to the nuclear compartment of C2C12 myoblasts following treatment with the nuclear export inhibitor leptomycin B (37). Other potential means of modulating the nuclear entry of δ-catenin exist. As we and others have indicated, signaling pools of p120-catenin subfamily members, including δ-catenin, appear to be subject to canonical Wnt signals or the pathway's destruction complex (63–66). For p120 itself (and δ-catenin?), this has an impact upon its nuclear presence/activity in a manner analogous to the key signal transducer β-catenin. Intriguingly, the Wnt11 ligand was recently reported to activate caspases in cardiomyocytes, resulting in suppression of β-catenin signaling and cardiac differentiation (67). Thus, differing Wnt ligands or contexts may conceivably have distinctive effects on p120-catenin subfamily members, wherein certain Wnts (or contexts) mediate stabilization of the catenin with consequent effects, whereas others engage caspases to generate catenin fragments capable of executing nuclear or other roles.

Our current study indicates that 817–1314, corresponding to a caspase-3 cleavage product, is efficiently enriched in the nucleus. We also found that δ-catenin (and 817–1314) binds to a novel zinc finger protein present in the nuclear compartment, ZIFCAT, belonging to the KRAB family. KRAB family zinc finger proteins make up a family of several hundred members, with the functions of most still to be determined. However, based on published studies, these proteins share features, including the presence of multiple zinc finger repeats within their carboxyl termini that directly bind DNA and, in our particular case with ZIFCAT, also δ-catenin. The amino-terminal KRAB domain in turn recruits cofactors, such as KAP1, to modulate gene transcription (57, 58).

Intriguingly, we further resolved the binding of ZIFCAT to ARVCF-catenin. Our *in vitro* and *in vivo* binding assays authenticated the interaction of ZIFCAT with δ-catenin and ARVCF. We have not yet tested whether this interaction extends to p120-catenin or, less likely, β-catenin, which belongs to a related but more distant catenin subfamily. If ZIFCAT is later found to bind p120 itself, it would be the third gene-regulatory protein (after Kaiso and Glis2) to bind p120 (38, 48).

Our initial characterization of ZIFCAT indicates that it is enriched in nuclei, binds to genomic DNA *in vitro*, and represses UAS-luciferase expression when fused to Gal4DBD. Neither δ-catenin nor ARVCF had an impact upon ZIFCAT (Gal4-UAS)-mediated reporter repression, probably because we showed that δ-catenin binds the zinc finger region of ZIFCAT, which bears little relevance in the artificial context employed (DNA binding being mediated via the Gal4DBD). *In vivo*, it is conceivable that δ-catenin (and/or ARVCF, etc.) may interfere with ZIFCAT binding to DNA, resulting in gene derepression (activation). Future work is needed to identify the DNA element(s) that ZIFCAT binds, so as to allow the testing of such models *in vivo* and *in vitro*. Further, identification of endogenous gene targets will be crucial in reaching an understanding of the nuclear activities of δ-catenin (and/or ARVCF, etc.) in conjunction with ZIFCAT. Additional work will also be necessary to determine the significance of caspase-3 cleavage in non-apoptotic processes, possibly, for example, the differentiation of stem cells where the caspase/catenin interaction was identified (49, 68). Collectively, our work may have revealed a novel signaling cascade triggered by caspase-3 cleavage of p120-catenin subfamily members, facilitating the coordinate modulation of cadherin, small GTPases, and nuclear functions.

Acknowledgments—We acknowledge Michelle C. Barton, Amy K. Sater, Lei Li, Warren S.-L. Liao, Malgorzata Kloc, and Shinako Takada for constructive comments as well as laboratory members Kyucheol Cho, Ji-Yeon Hong, Rachel K. Miller, and William A. Munoz for helpful discussions.

REFERENCES

1. Logan, C. Y., and Nusse, R. (2004) *Annu. Rev. Cell Dev. Biol.* **20,** 781–810
2. MacDonald, B. T., Tamai, K., and He, X. (2009) *Dev. Cell* **17,** 9–26
3. Artavanis-Tsakonas, S., Rand, M. D., and Lake, R. J. (1999) *Science* **284,** 770–776
4. Moon, R. T., Kohn, A. D., De Ferrari, G. V., and Kaykas, A. (2004) *Nat. Rev. Genet.* **5,** 691–701
5. Hansson, E. M., Lendahl, U., and Chapman, G. (2004) *Semin. Cancer Biol.* **14,** 320–328
6. Harris, T. J., and Tepass, U. (2010) *Nat. Rev. Mol. Cell Biol.* **11,** 502–514
7. Gumbiner, B. M. (2005) *Nat. Rev. Mol. Cell Biol.* **6,** 622–634
8. Yap, A. S., and Kovacs, E. M. (2003) *J. Cell Biol.* **160,** 11–16
9. Jeanes, A., Gottardi, C. J., and Yap, A. S. (2008) *Oncogene* **27,** 6920–6929
10. Reynolds, A. B., and Carnahan, R. H. (2004) *Semin. Cell Dev. Biol.* **15,** 657–663
11. Steinhusen, U., Badock, V., Bauer, A., Behrens, J., Wittman-Liebold, B., Dörken, B., and Bommert, K. (2000) *J. Biol. Chem.* **275,** 16345–16353
12. Senthivinayagam, S., Mishra, P., Paramasivam, S. K., Yallapragada, S., Chatterjee, M., Wong, L., Rana, A., and Rana, B. (2009) *J. Biol. Chem.* **284,** 13577–13588
13. Kessler, T., and Müller, H. A. (2009) *BMC Dev. Biol.* **9,** 15
14. Brancolini, C., Lazarevic, D., Rodriguez, J., and Schneider, C. (1997) *J. Cell Biol.* **139,** 759–771
15. Cirillo, N., Lanza, M., De Rosa, A., Cammarota, M., La Gatta, A., Gombos, F., and Lanza, A. (2008) *J. Cell. Biochem.* **103,** 598–606
16. Dusek, R. L., Getsios, S., Chen, F., Park, J. K., Amargo, E. V., Cryns, V. L., and Green, K. J. (2006) *J. Biol. Chem.* **281,** 3614–3624
17. Hunter, I., McGregor, D., and Robins, S. P. (2001) *J. Bone Miner. Res.* **16,** 466–477
18. Steinhusen, U., Weiske, J., Badock, V., Tauber, R., Bommert, K., and Huber, O. (2001) *J. Biol. Chem.* **276,** 4972–4980
19. Herren, B., Levkau, B., Raines, E. W., and Ross, R. (1998) *Mol. Biol. Cell* **9,**

Downloaded from www.jbc.org at HAM-TMC Library, on January 31, 2013

1589–1601
20. Weiske, J., and Huber, O. (2005) *Methods Mol. Biol.* **289,** 175–192
21. Ling, Y., Zhong, Y., and Perez-Soler, R. (2001) *Mol. Pharmacol.* **59,** 593–603
22. Feinstein-Rotkopf, Y., and Arama, E. (2009) *Apoptosis* **14,** 980–995
23. Kuranaga, E., and Miura, M. (2007) *Trends Cell Biol.* **17,** 135–144
24. Zheng, G., Lyons, J. G., Tan, T. K., Wang, Y., Hsu, T. T., Min, D., Succar, L., Rangan, G. K., Hu, M., Henderson, B. R., Alexander, S. I., and Harris, D. C. (2009) *Am. J. Pathol.* **175,** 580–591
25. McCusker, C. D., and Alfandari, D. (2009) *Commun. Integr. Biol.* **2,** 155–157
26. Parisiadou, L., Fassa, A., Fotinopoulou, A., Bethani, I., and Efthimiopoulos, S. (2004) *Neurodegener. Dis.* **1,** 184–191
27. Ferber, E. C., Kajita, M., Wadlow, A., Tobiansky, L., Niessen, C., Ariga, H., Daniel, J., and Fujita, Y. (2008) *J. Biol. Chem.* **283,** 12691–12700
28. Suzanne, M., and Steller, H. (2009) *J. Biol.* **8,** 49
29. McCrea, P. D., and Gu, D. (2010) *J. Cell Sci.* **123,** 637–642
30. Reynolds, A. B. (2007) *Biochim. Biophys. Acta* **1773,** 2–7
31. Xiao, K., Oas, R. G., Chiasson, C. M., and Kowalczyk, A. P. (2007) *Biochim. Biophys. Acta* **1773,** 8–16
32. Anastasiadis, P. Z. (2007) *Biochim. Biophys. Acta* **1773,** 34–46
33. Abu-Elneel, K., Ochiishi, T., Medina, M., Remedi, M., Gastaldi, L., Caceres, A., and Kosik, K. S. (2008) *J. Biol. Chem.* **283,** 32781–32791
34. Matter, C., Pribadi, M., Liu, X., and Trachtenberg, J. T. (2009) *Neuron* **64,** 320–327
35. Kim, K., Sirota, A., Chen Yh, Y. H., Jones, S. B., Dudek, R., Lanford, G. W., Thakore, C., and Lu, Q. (2002) *Exp. Cell Res.* **275,** 171–184
36. Gu, D., Sater, A. K., Ji, H., Cho, K., Clark, M., Stratton, S. A., Barton, M. C., Lu, Q., and McCrea, P. D. (2009) *J. Cell Sci.* **122,** 4049–4061
37. Rodova, M., Kelly, K. F., VanSaun, M., Daniel, J. M., and Werle, M. J. (2004) *Mol. Cell. Biol.* **24,** 7188–7196
38. Daniel, J. M. (2007) *Biochim. Biophys. Acta* **1773,** 59–68
39. Kosik, K. S., Donahue, C. P., Israely, I., Liu, X., and Ochiishi, T. (2005) *Trends Cell Biol.* **15,** 172–178
40. Arikkath, J., Peng, I. F., Ng, Y. G., Israely, I., Liu, X., Ullian, E. M., and Reichardt, L. F. (2009) *J. Neurosci.* **29,** 5435–5442
41. Israely, I., Costa, R. M., Xie, C. W., Silva, A. J., Kosik, K. S., and Liu, X. (2004) *Curr. Biol.* **14,** 1657–1663
42. Zhang, J. Y., Wang, Y., Zhang, D., Yang, Z. Q., Dong, X. J., Jiang, G. Y., Zhang, P. X., Dai, S. D., Dong, Q. Z., Han, Y., Zhang, S., Cui, Q. Z., and Wang, E. H. (2010) *J. Pathol.* **222,** 76–88
43. Zeng, Y., Abdallah, A., Lu, J. P., Wang, T., Chen, Y. H., Terrian, D. M., Kim, K., and Lu, Q. (2009) *Mol. Cancer* **8,** 19
44. Lu, Q., Zhang, J., Allison, R., Gay, H., Yang, W. X., Bhowmick, N. A., Frelix, G., Shappell, S., and Chen, Y. H. (2009) *Prostate* **69,** 411–418
45. Kornbluth, S., and Evans, E. K. (2001) *Current Protocols in Cell Biology*, Chapter 11, Unit 11.12, John Wiley & Sons, Inc., New York
46. Schreiber, E., Matthias, P., Müller, M. M., and Schaffner, W. (1989) *Nucleic Acids Res.* **17,** 6419
47. Fang, X., Ji, H., Kim, S. W., Park, J. I., Vaught, T. G., Anastasiadis, P. Z., Ciesiolka, M., and McCrea, P. D. (2004) *J. Cell Biol.* **165,** 87–98
48. Hosking, C. R., Ulloa, F., Hogan, C., Ferber, E. C., Figueroa, A., Gevaert, K., Birchmeier, W., Briscoe, J., and Fujita, Y. (2007) *Mol. Biol. Cell* **18,** 1918–1927
49. Dejosez, M., Krumenacker, J. S., Zitur, L. J., Passeri, M., Chu, L. F., Songyang, Z., Thomson, J. A., and Zwaka, T. P. (2008) *Cell* **133,** 1162–1174
50. Fishman, J. A., and Karnovsky, M. J. (1985) *Am. J. Pathol.* **118,** 398–407
51. Davidoff, A. N., and Mendelow, B. V. (1992) *Leuk. Res.* **16,** 1077–1085
52. Solary, E., Eymin, B., Droin, N., and Haugg, M. (1998) *Cell Biol. Toxicol.* **14,** 121–132
53. Heasman, S. J., and Ridley, A. J. (2008) *Nat. Rev. Mol. Cell Biol.* **9,** 690–701
54. DeBusk, L. M., Boelte, K., Min, Y., and Lin, P. C. (2010) *J. Exp. Med.* **207,** 77–84
55. Martinez, M. C., Ochiishi, T., Majewski, M., and Kosik, K. S. (2003) *J. Cell Biol.* **162,** 99–111
56. Lu, Q., Paredes, M., Medina, M., Zhou, J., Cavallo, R., Peifer, M., Orecchio, L., and Kosik, K. S. (1999) *J. Cell Biol.* **144,** 519–532
57. Looman, C., Abrink, M., Mark, C., and Hellman, L. (2002) *Mol. Biol. Evol.* **19,** 2118–2130
58. Urrutia, R. (2003) *Genome Biol.* **4,** 231
59. Lockshin, R. A., and Zakeri, Z. (2007) *J. Cell Mol. Med.* **11,** 1214–1224
60. Kumar, S. (2007) *Cell Death Differ.* **14,** 32–43
61. Kim, K., Pang, K. M., Evans, M., and Hay, E. D. (2000) *Mol. Biol. Cell* **11,** 3509–3523
62. Lu, J. P., Zhang, J., Kim, K., Case, T. C., Matusik, R. J., Chen, Y. H., Wolfe, M., Nopparat, J., and Lu, Q. (2010) *Mol. Cancer* **9,** 304
63. Hong, J. Y., Park, J. I., Cho, K., Gu, D., Ji, H., Artandi, S. E., and McCrea, P. D. (2010) *J. Cell Sci.* **123,** 4351–4365
64. Bareiss, S., Kim, K., and Lu, Q. (2010) *J. Neurosci. Res.* **88,** 2350–2363
65. Oh, M., Kim, H., Yang, I., Park, J. H., Cong, W. T., Baek, M. C., Bareiss, S., Ki, H., Lu, Q., No, J., Kwon, I., Choi, J. K., and Kim, K. (2009) *J. Biol. Chem.* **284,** 28579–28589
66. Park, J. I., Ji, H., Jun, S., Gu, D., Hikasa, H., Li, L., Sokol, S. Y., and McCrea, P. D. (2006) *Dev. Cell* **11,** 683–695
67. Abdul-Ghani, M., Dufort, D., Stiles, R., De Repentigny, Y., Kothary, R., and Megeney, L. A. (2011) *Mol. Cell. Biol.* **31,** 163–178
68. Fujita, J., Crane, A. M., Souza, M. K., Dejosez, M., Kyba, M., Flavell, R. A., Thomson, J. A., and Zwaka, T. P. (2008) *Cell Stem Cell* **2,** 595–601

Downloaded from www.jbc.org at HAM-TMC Library, on January 31, 2013